THE GEOLOGICAL SOCIETY OF AMERICA®

When "evaporites" are not formed by evaporation: The role of temperature and pCO_2 on saline deposits of the Eocene Green River Formation, Colorado, USA

Robert V. Demicco† and Tim K. Lowenstein
Department of Geological Sciences and Environmental Studies, Binghamton University, Binghamton, New York 13902-6000, USA

ABSTRACT

Halite precipitates in the Dead Sea during winter but re-dissolves above the thermocline upon summer warming, "focusing" halite deposition below the thermocline (Sirota et al., 2016, 2017, 2018). Here we develop an "evaporite focusing" model for evaporites (nahcolite + halite) preserved in a restricted area of the Eocene Green River Formation in the Piceance Creek Basin of Colorado, USA. Nahcolite solubility is dependent on partial pressure of carbon dioxide (pCO_2) as well as temperature (T), so these models covary with both T and pCO_2. In the lake that filled the Piceance Creek Basin, halite, nahcolite or mixtures of both could have precipitated during winter cooling, depending on the CO_2 content in different parts of the lake. Preservation of these minerals occurs below the thermocline (>~25 m) in deeper portions of the basin. Our modeling addresses both: (1) the restriction of evaporites in the Piceance Creek Basin to the center of the basin without recourse to later dissolution and (2) the variable mineralogy of the evaporites without recourse to changes in lake water chemistry. T from 20 to 30 °C and pCO_2 between 1800 and 2800 ppm are reasonable estimates for the conditions in the Piceance Creek Basin paleolake. Other evaporites occur in the center of basins but do not extend out to the edges of the basin. Evaporite focusing caused by summer-winter T changes in the solubility of the minerals should be considered for such deposits and variable pCO_2 within the evaporating brines also needs to be considered if pCO_2 sensitive minerals are found.

INTRODUCTION

Geologists studying salt deposits have noticed that very soluble minerals that occur in the center of a basin do not extend out to the edges of the basin (Hsü et al., 1973; Dyni, 1981; Lowenstein, 1988). This is true even where: (1) soluble salts are interpreted to have been deposited in a deep evaporitic lake or marine basin and (2) deep-water deposits that encase salts in the center of the basin can be confidently traced to peripheral deposits. This situation is a hallmark of the Parachute Creek Member of the Green River Formation in the Piceance Creek Basin of northwestern Colorado, USA (Fig. 1). The Parachute Creek Member, up to ~900 m thick, comprises dolomitic and siliceous mudstones, including oil shale, that contain bedded and disseminated evaporites formed in a perennial saline lake during the early Eocene climatic optimum (EECO) 52–50 Ma (Dyni 1981, 1996; Lowenstein and Demicco, 2006; Smith et al., 2008; Tänavsuu-Milkeviciene and Sarg, 2012; Jagniecki and Lowenstein, 2015; Jagniecki et al., 2015). The eroded remains of the lacustrine oil shale deposits of the Parachute Creek Member in the Piceance Creek Basin cover more than 4500 km^2, whereas the evaporites in the north central portion of the basin are confined to an area in the subsurface of only 700 km^2 (Fig. 1A). Dyni (1981) argued that the evaporites had originally extended over a considerably larger area and had been subsequently leached by fresh groundwaters recharging the basin (Fig. 1B), an explanation commonly invoked for the Parachute Creek Member (cf. plates 1 and 2 *in* Johnson and Brownfield, 2015).

Recent work on halite deposition in the modern Dead Sea by Sirota et al. (2016, 2017, 2018) has documented what those authors refer to as "halite focusing." The precipitation of halite is triggered by falling water temperatures (T) during the winter months when the entire Dead Sea becomes isothermal at ~24 °C and supersaturated with halite. During summer, the waters of the lake above the thermocline (at <25 m depth) warm to ~34 °C, become undersaturated with halite due to the temperature increase, and the bulk of the winter-deposited halite above the thermocline re-dissolves. Summer dissolution of halite occurs in the Dead Sea despite any increase in evaporative concentration at the surface. The halite that settled into the deeper, cooler isothermal bottom waters, however, accumulates as an annual layer at depths below the 25 m deep thermocline, which "focuses" halite deposition into the deeper portions of the Dead Sea. Continued evaporative concentration, caused by a negative water balance in the basin, sets up the lake for the next annual cycle.

The purpose of this paper is to apply a modified version of the "halite focusing" model to the Parachute Creek Member of the Green River Formation in the Piceance Creek Basin. However, the situation for the Parachute Creek Member is complicated by the fact that two evaporite minerals, nahcolite ($NaHCO_3$) and halite, occur as laminae in the center of the basin. Halite-nahcolite laminae and thin beds from the Parachute Creek Member have variable compositions within and between layers (Fig. 2). There are layers of pure nahcolite crystal mud; layers of pure halite as millimeter-diameter cumulate cubes, surface-formed rafts together with cumulate cubes, and larger, upward-oriented halite crystals that grew off the floor of the lake. Significantly, many layers contain nahcolite crystal mud and halite cubes and rafts in varying proportions (see Jagniecki and Lowenstein, 2015, for further details). The addition of nahcolite to the evaporites in the Parachute Creek Member adds two complexities. First, nahcolite and halite share a common component, Na, so if either halite or nahcolite precipitates, the activity (concentration) of Na in the brine will decrease and affect the saturation state of the other mineral. Second, unlike halite, nahcolite solubility

†demicco@binghamton.edu.

 https://doi.org/10.1130/B35303.1; 11 figures; 1 table.

is notably dependent on both T and partial pressure of carbon dioxide (pCO_2) in the brine. This fact formed the basis of the "nahcolite proxy" (Eugster, 1966; Lowenstein and Demicco, 2006; Jagniecki et al., 2015). In these studies, the finely laminated, finely crystalline nahcolite in the Piceance Creek Basin was interpreted to have formed from a brine in equilibrium with atmospheric pCO_2 which constrained EECO atmospheric pCO_2 at >680 ppm depending on the temperature of the brine.

The fact that the solubility of carbonate minerals is dependent on the pCO_2 in the brine as well as temperature also suggests that, if different parts of a lake with very nearly the same brine chemistry come into equilibrium with different pCO_2 or temperature, the solubility of those carbonate minerals and halite (which shares Na with those minerals) might be affected. Here we develop a modified "evaporite focusing" model using numerical simulations with the programs EQL/EVP (Risacher and Clement, 2001) and FREZCHEM (Marion, 2001). We show that, in the Piceance Creek Basin, natural variations of total dissolved CO_2 in different parts of the ancient lake coupled with summer-winter variations in temperature of these different parts of the lake were capable

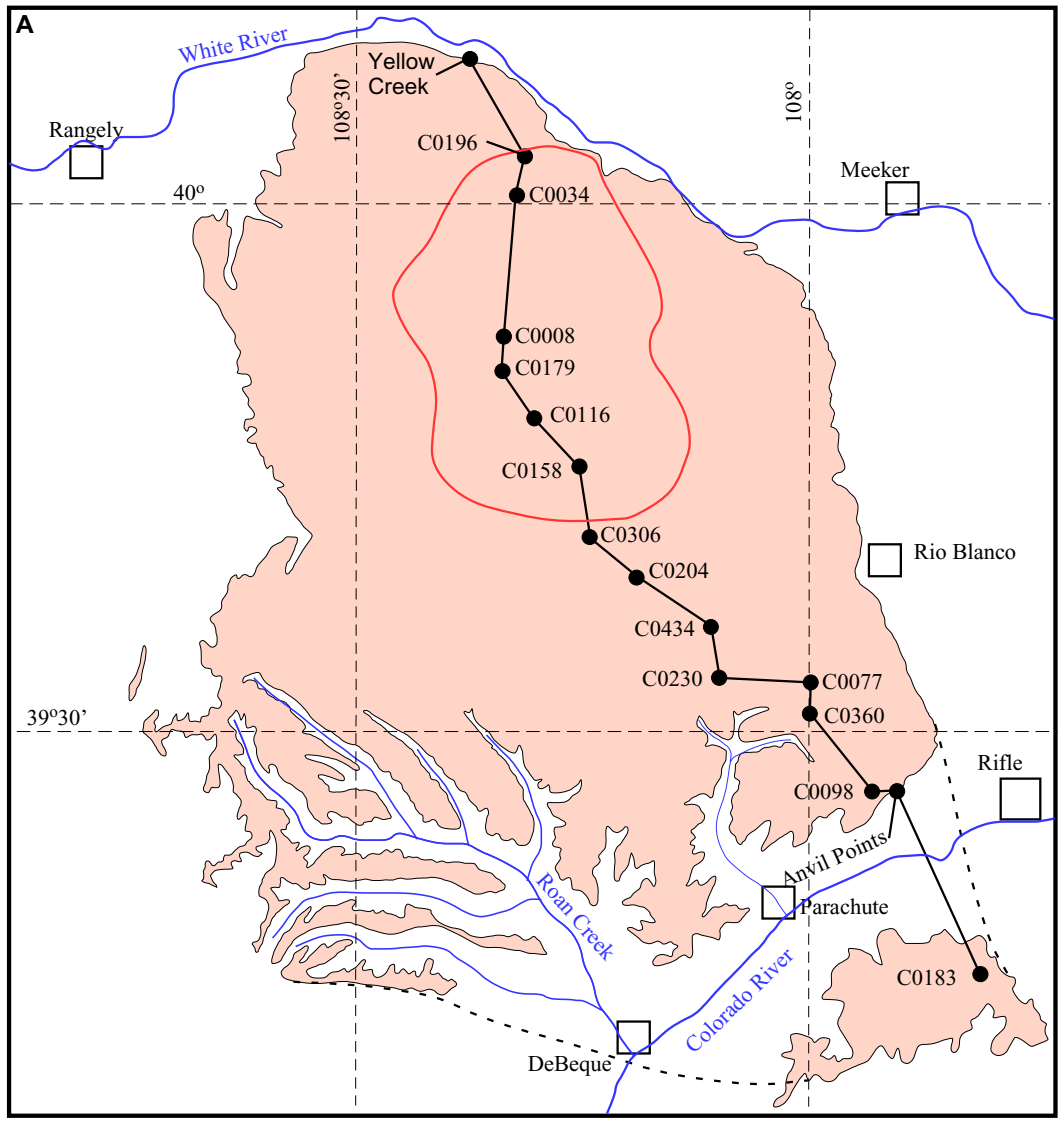

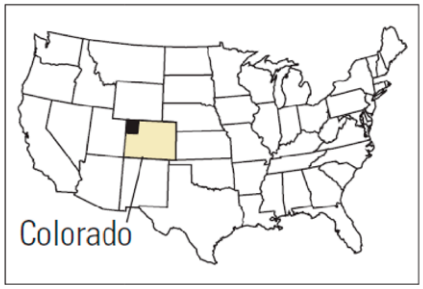

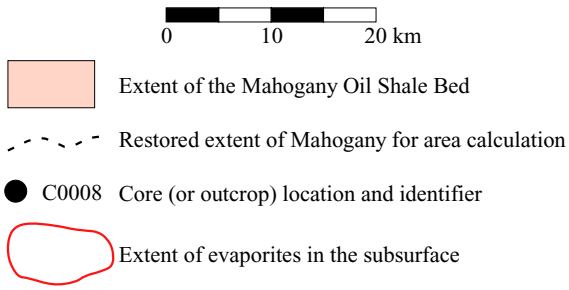

Figure 1 (*on this and following page*). Eocene Green River Formation deposits in the Piceance Creek Basin of northwestern Colorado, USA. (A) Map outlining the extent of the Mahogany Bed, an organic-rich carbonate mudstone ("oil shale") found at the top of the Parachute Creek Member of the Green River Formation. The much smaller area outlined by the red line shows the extent of the evaporites in the subsurface (modified from Brownfield et al., 2010a). Surface outcrops (labeled) and wells (C0 numbers) comprise the cross section in B.

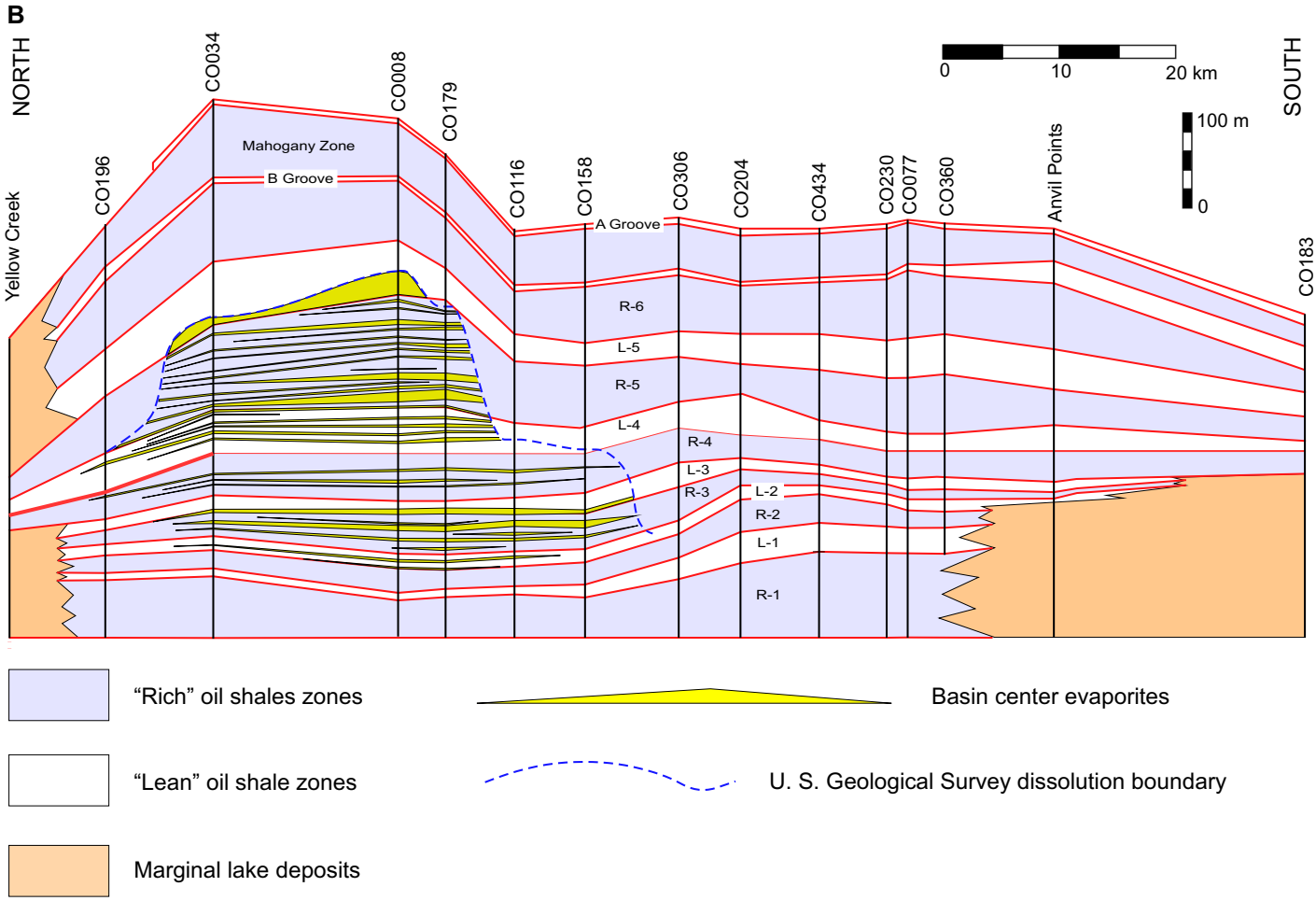

Figure 1 (*Continued*). (B) Roughly north to south cross section through the Parachute Creek Member (and laterally equivalent basin margin deposits) in the Piceance Creek Basin (modified from Johnson and Brownfield, 2015). Evaporites (halite and nahcolite) shown in yellow. Rich oil shale zones are commonly interpreted as deep, anoxic lake deposits. In the interpretation shown here, evaporites once extended an unknown distance out away from where they are now preserved and were removed later in the history of the basin by groundwater dissolution. However, there is no evidence of dissolved halite and nahcolite beds in the Yellow Creek outcrop, the Anvil Points outcrop, or other outcrops.

of driving precipitation of laminae with various relative amounts of nahcolite and halite (Fig. 2) during winter cooling. Where these laminae accumulated below the thermocline, they were preserved whereas above the thermocline, both nahcolite and halite dissolved as the shallower waters warmed up during summer. This modified evaporite focusing model solves two problems: (1) the restriction of nahcolite and halite in the Parachute Creek Member to a small area of the Piceance Creek Basin and (2) the distinctive variations in the mineralogy and thicknesses of the evaporite layers in the basin center. The evaporite focusing model also has implications for the depth of the lake that deposited the Parachute Creek Member.

MODEL DEVELOPMENT

Figure 3 shows the stability fields of nahcolite, trona, and natron as a function of pCO_2 and temperature. It is a modified version of the experimental results of Jagniecki et al. (2015) (their fig. 3). Minerals and solution are in equilibrium with gas at 1 atmosphere total pressure. Phase boundaries were calculated from derived thermochemical data. The dashed black line is the boundary between nahcolite and trona where the brine is at halite saturation.

Lake Magadi, in the rift basin of Kenya, is considered to be a close chemical analog for the ancient lake that deposited the Parachute Creek Member in the Piceance Creek Basin (Jagniecki and Lowenstein, 2015). Modern lakes that precipitate sodium carbonate minerals are rare and require a unique Na, CO_2 enriched chemistry (Lowenstein et al., 2017). The brine used in the numerical experiments described below was the average of 25 modern surface brines, charge-balanced, from Lake Magadi (Table 1; Eugster, 1970; Jones et al., 1977). This brine composition was $Na^+ = 4.98$ mol/kg(H_2O); $K^+ = 0.040$ mol/kg(H_2O); $Ca^{2+} = 0$ mol/kg(H_2O); $Mg^{2+} = 0$ mol/kg(H_2O); $Cl^- = 1.91$ mol/kg(H_2O); $SO_4^{2-} = 0.015$ mol/kg(H_2O); alkalinity = 3.08 mol/kg(H_2O) (where alkalinity is defined as mol/kg(H_2O)$HCO_3^- + 2$*mol/kg(H_2O)CO_3^{2-}); with a calculated pH = 9.9 (measured pHs given in Table 1). The density of this brine is ~1230 kg m^{-3} (Table 1). The negligible concentrations of calcium and magnesium reflect the fact that Lake Magadi brines have already evolved through the so-called "carbonate chemical divide" (Hardie and Eugster, 1970).

Whereas Lake Magadi is considered to be a close chemical analog for the ancient lake that deposited the Parachute Creek Member in the Piceance Creek Basin, the Dead Sea is herein considered to be the closest modern physical analog of that lake in terms of evaporite deposition driven by winter-summer temperature variations.

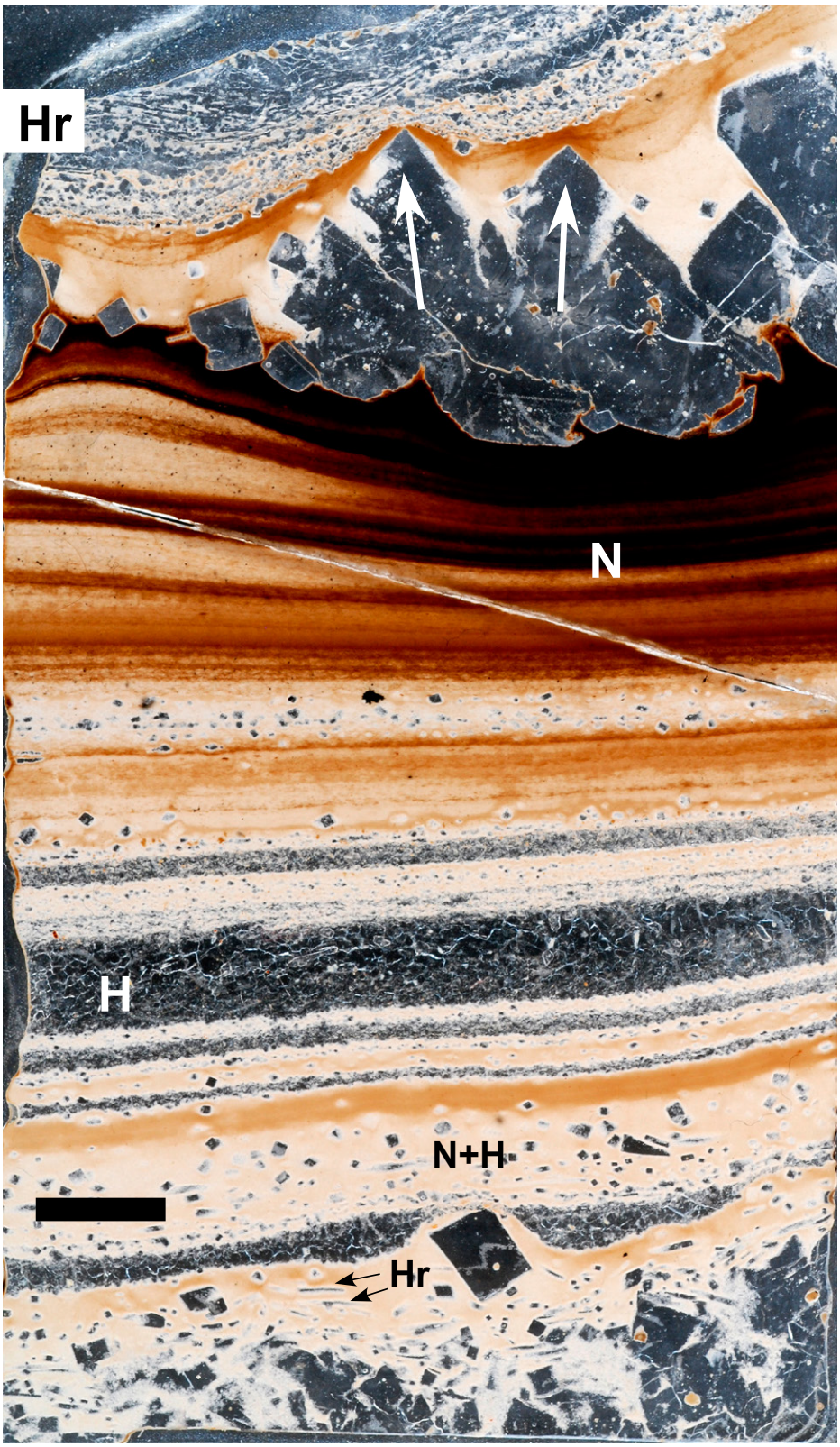

Figure 2. Thin-section photomicrograph of primary nahcolite and halite from the Parachute Creek Member in the Piceance Creek Basin of northwestern Colorado, USA (fig. DR2 from Jagniecki et al., 2015). Laminae display a variety of textures diagnostic of precipitation in a perennial, density-stratified, saline lake. Nahcolite (N) occurs as light brown to black, organic-rich laminae composed of mud-sized crystals interpreted to have precipitated within the water column in winter. Halite (H) occurs as clear crystalline layers in the middle of the thin section and as larger cubes at the bottom and the top of the thin section. Nahcolite + halite laminae (N + H) contain halite cubes and platy "rafts" (Hr and small black arrows). The rafts indicate those halite crystals originally precipitated at the air-water interface and sank to the lake bottom to form layered accumulations. Fine nahcolite + halite crystal muds drape upward-widening halite crystals (denoted by the white arrows) that formed at the bottom of the brine. Scale bar 5 mm long. Thin section from a depth of 561 m from the Shell 23x-2 well (core C0179 on Fig. 1).

The annual summer-winter temperature cycle in the Dead Sea (located at 31.5°N latitude) is ~36 to ~24 °C. Moreover, temperatures of fluid inclusions from bottom growth halite in the Piceance Creek Basin show trapping temperatures of ~21–28 °C with a strong mode between 20 and 25 °C (LaClair and Lowenstein, 2009). We used the surface temperatures from the modern Dead Sea and the fluid inclusions from the bottom-growth halite from the Piceance Creek Basin as guidelines to design an initial experiment in which T varied from 20 to 30 °C to simulate winter-sum-

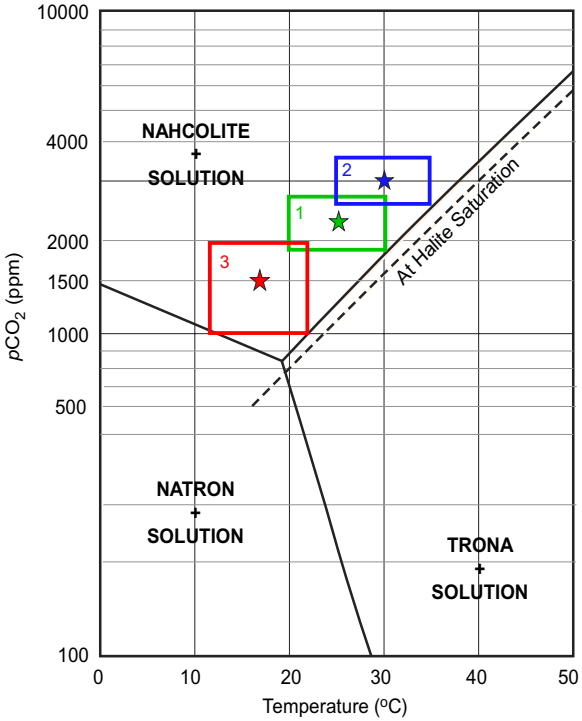

Figure 3. The stability fields of nahcolite, trona, and natron as a function of partial pressure of carbon dioxide (pCO_2) and temperature (T) modified from experimental results of Jagniecki et al., 2015 (their fig. 3). Minerals and solution are in equilibrium with gas at 1 atmosphere total pressure. Phase boundaries were calculated from derived thermochemical data. Dashed black line is the boundary between nahcolite and trona where the brine is at halite saturation. The three boxes outline the conditions of numerical experiments where Lake Magadi, Kenya, brine was evaporated to saturation with nahcolite or nahcolite + halite at the T and pCO_2 conditions in the center of a box (star). The evaporated brines were then systematically re-equilibrated with different T and pCO_2 within the bounds of the box. The conditions were: (1) green box, T ± 5 °C from 25 °C, ±500 ppm from 2300 ppm pCO_2; (2) blue box, T ± 5 °C from 30 °C, ±500 ppm from 2300 ppm pCO_2; and (3) red box, T ± 5 °C from 17 °C, ±500 ppm from 1500 ppm pCO_2. The fields were chosen to keep the re-equilibrated brines within the stability field of nahcolite.

mer temperature changes. The object of these experiments was to supersaturate lake waters with halite and nahcolite during winter (temperatures of 20–25 °C) and under saturate lake waters with respect to nahcolite and halite in summer (temperatures >25 °C) to model winter precipitation and summer dissolution. The pCO_2 range for this experiment is harder to determine as there are virtually no direct measurements of dissolved pCO_2 in modern lakes, let alone modern alkaline saline lakes such as the one that deposited the Parachute Creek Member. However, the T range of the initial experiment fixes a minimum pCO_2 at 1800 ppm (Fig. 3; also see Jagniecki et al., 2105). If the pCO_2 were to fall below that limit, at higher temperatures the experiments would put the brines into the trona field at initial sodium carbonate mineral precipitation. And neither trona nor trona pseudomorphs are known from the Piceance Creek Basin. We arbitrarily chose a 1000 ppm variation of pCO_2 so the green box in Figure 3 outlines the conditions of the initial experiment: (1) T ranges from 20 to 30 °C and (2) pCO_2 from 1800 to 2800 ppm. The red and blue boxes in Figure 3 show the conditions of two additional numerical experiments with 10 °C temperature changes and a 1000 ppm pCO_2 change: (1) blue box (25–35 °C T range: 2600–3600 ppm pCO_2 range) and (2) red box (12–22 °C T range: 1000–2000 ppm pCO_2 range).

TABLE 1. TWENTY-FIVE ANALYSES OF LAKE MAGADI, KENYA, SURFACE BRINES (EUGSTER, 1970; JONES ET AL., 1977) AND THE MEAN USED IN THIS STUDY, GREEN RIVER FORMATION, COLORADO, USA (AFTER CHARGE BALANCE ON NA AND CO_3)

TDS	Density	T	pH	Na	K	Ca	Mg	Alkalinity	Cl + F
145000	1.14	27	9.4	2.77	0.028	0	0	1.96	0.83
193000	1.18	25	9.8	3.62	0.026	0	0	2.5	1.13
218000	1.2	30	9.5	4.02	0.027	0	0	2.92	1.11
237000	1.22	25	9.9	4.22	0.04	0	0	2.8	1.44
238000	1.22	30	10.1	4.46	0.03	0	0	3	1.46
247000	1.23	36	9.8	4.54	0.04	0	0	3.01	1.55
257000	1.24	42	10.3	4.76	0.034	0	0	3.08	1.68
257000	1.24	38	10.3	4.8	0.034	0	0	3.12	1.69
258000	1.24	41	10.2	4.94	0.04	0	0	3.39	1.57
267000	1.25	26	10.5	4.99	0.038	0	0	3.24	1.75
279000	1.26	30	10.7	5.06	0.054	0	0	2.45	2.62
290000	1.27	26	10.5	5.33	0.051	0	0	3.43	1.93
290000	1.27	38	10.5	5.35	0.043	0	0	3.43	1.92
291000	1.27	0	10.5	5.24	0.058	0	0	2.4	2.85
285000	1.27	28	10.5	5.44	0.046	0	0	3.49	1.94
313000	1.29	40	10.7	5.28	0.046	0	0	3.11	2.18
293000	1.28	25	10.5	5.47	0.04	0	0	3.55	1.92
312000	1.29	38	9.9	5.7	0.051	0	0	3.12	2.58
319000	1.3	31	10.8	5.7	0.052	0	0	3.17	2.51
317000	1.3	34	10.7	5.69	0.052	0	0	3.28	2.42
321000	1.3	39	10.4	5.75	0	0	0	3.18	2.51
305000	1.29	26	10.6	5.87	0.047	0	0	3.73	2.15
306000	1.29	27	10.6	5.73	0.049	0	0	3.33	2.34
316260	1.3	52	10.7	5.78	0.052	0	0	3.29	2.5
218000	1.2	30	9.5	4.02	0.027	0	0	2.92	1.11
			9.9	4.98	0.04	0	0	3.08	1.91

Note: T—temperature in °C.

Experiment 1: T 20–30 °C–pCO_2 1800–2800 ppm

What is hinted at in Figure 3, but not explicitly shown, is that the stability fields of the sodium carbonate minerals are also dependent on the activity of H_2O (aH_2O). Figure 4 is a full, three-dimensional plot that shows two surfaces defined by explicit conditions of T, pCO_2, and aH_2O that control the mineralogy (natron, nahcolite, or trona) obtained at those conditions. The lower tri-colored surface shows which sodium carbonate mineral first forms as a brine of the specified composition is evaporated, causing the aH_2O to decrease. Where viewed perpendicular to the aH_2O axis, and projected down onto the base of the figure, this lower tri-colored surface reproduces Figure 3, albeit in a different orientation. The upper surface (at much lower aH_2O indicating substantial evaporation of the brine) shows the T, pCO_2, and aH_2O conditions at the first appearance of halite. At halite saturation, the nahcolite and trona field areas have substantially enlarged at the expense of natron. And the boundary between the nahcolite and trona fields has shifted and now conforms to the position of the dashed line in Figure 3. This figure was prepared with EQL/EVP (Risacher and Clement, 2001) by evaporating the Lake Magadi brine up to the first appearance of a sodium carbonate phase under various combinations of T (ranging from 0 to 50 °C) and pCO_2 (100–10,000 ppm) and then continuing the evaporation of that brine to the first appearance of halite. We modified the database files in EQL/EVP to use the new experimental thermodynamic data of Jagniecki et al. (2015) for trona, natron, and nahcolite.

It is important to note that at every point on these surfaces: (1) the brine is saturated with the designated phase(s), (2) the mol/kg of all of the ions and ion complexes in the brine is slightly different, and (3) the masses of any sodium

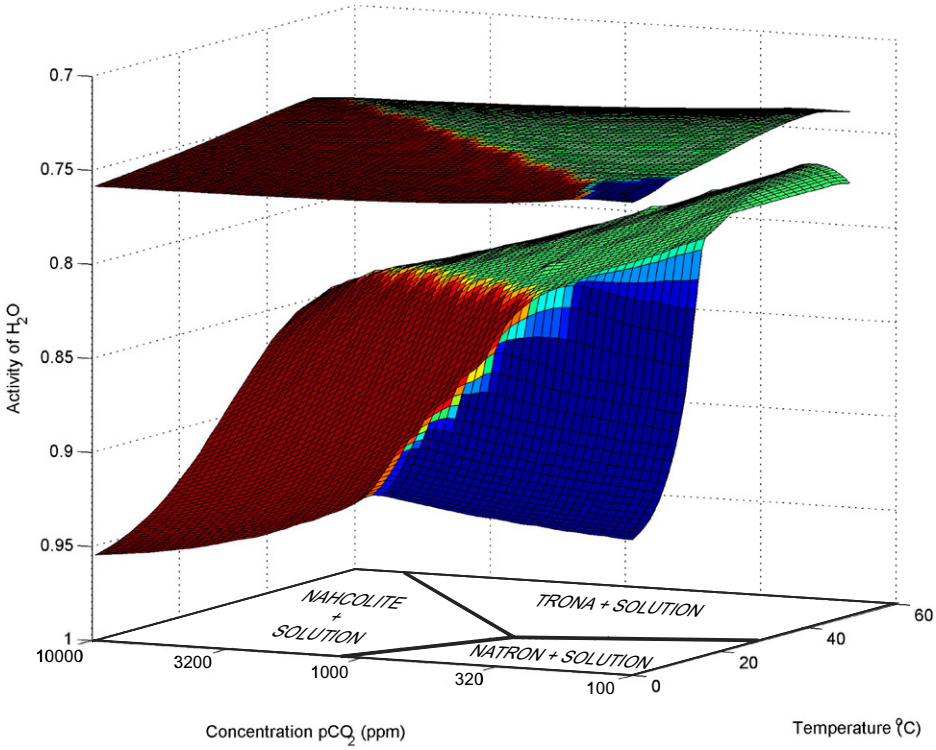

Figure 4. Three-dimensional plot calculated with EQL/EVP (Risacher and Clement, 2001) of temperature (T), partial pressure of carbon dioxide (pCO_2), and activity of H_2O (aH_2O) showing two tri-colored surfaces that correspond to features of Figure 3. The lower surface shows the sodium carbonate mineral (natron—blue; nahcolite—red; trona—green) that first forms as the Lake Magadi, Kenya, brine was evaporated. Where viewed perpendicular to the aH_2O axis, this lower surface reproduces Figure 1 as outlined on the base of the diagram. The upper surface (at much lower aH_2O indicating substantial evaporation of the brine) shows the T, pCO_2, aH_2O conditions and stable sodium carbonate mineral at the first appearance of halite. Note that, at halite saturation, the nahcolite and trona fields have substantially enlarged at the expense of natron. The boundary between the nahcolite and trona fields has shifted and now conforms to the position of the dashed line in Figure 1.

carbonate mineral ± halite precipitated are also slightly different. These three facts are the basis of the argument developed in this paper.

Initial Precipitation of Nahcolite

Figure 5A shows the lower surface of Figure 4: the T, pCO_2, and aH_2O conditions at the first appearance of one of three sodium carbonate phases: natron (blue), nahcolite (red), and trona (green) as the Lake Magadi brine is evaporated. The yellow lines on Figure 3 show: (1) a line of constant pCO_2 (2300 ppm) with T ranging from 0 to 50 °C and (2) a line of constant T (25 °C) with pCO_2 ranging from 100 to 10,000 ppm. These lines cross at the point 25 °C, 2300 ppm pCO_2 (the center of the white box in Fig. 5A). The white box in Figure 5A is the same as the green box in Figure 3 but warped to fit on the aH_2O surface. Figure 5B is a blowup of the region outlined by the white box in Figure 5A. At the point where the lines cross, the mol/kg H_2O of Na, K, Cl, SO_4, and OH are fixed as is the alkalinity, and the pH. And this is true for every other point on the surface, each of which has its own unique concentrations of ions. However, above that surface, the saturation states of natron, nahcolite, and trona are not at all obvious, but they can be calculated with the program FREZCHEM52 (Marion, 2001). Unlike EQL/EVP, FREZCHEM was designed to easily calculate mineral equilibria with changing T and can be easily modified to consider changes in pCO_2 as well. As with EQL/EVP, we modified the database files in FREZCHEM to use the experimental thermodynamic data of Jagniecki et al. (2015) for trona, natron, and nahcolite.

We input the brine composition at 25 °C, 2300 ppm CO_2, where nahcolite first precipitates, into FREZCHEM and: (1) changed temperature from 30 to 20 °C at constant pCO_2 concentration of 2300 ppm and (2) changed pCO_2 concentrations from 1800 to 2800 ppm at a constant temperature of 25 °C. The results are displayed in the left and right panels or in Figure 5C, respectively. These two experiments correspond to the yellow lines in Figure 5B. In the bottom panels of Figure 5C, the heavy black lines are the Ksp (dimensionless equilibrium constant at the appropriate T and pCO_2) for nahcolite and the red dotted lines are the appropriate ion activity product (IAP—also dimensionless) for [$a\mathrm{Na}^{+}{*}a\mathrm{HCO}_3^{-}$], both calculated by FREZCHEM. In the lower left panel of Figure 5C, as temperature decreases, the IAP increases until it equals the Ksp at 25 °C. If nahcolite (or another sodium carbonate mineral) could not precipitate, the IAP would continue to increase along that trajectory as T decreased. However, when nahcolite is precipitated below 25 °C, then the IAP = Ksp. And, the lower the

Figure 5. Numerical experiment 1 (green box in Fig. 3): nahcolite saturation. (A) The temperature (T), partial pressure of carbon dioxide (pCO_2), and activity of H_2O (aH_2O) conditions of the first appearance of a sodium carbonate phase with evaporation of the Lake Magadi, Kenya, brine (lower surface in Fig. 4). Yellow lines are constant T (25 °C) with variable pCO_2 (100–10,000 ppm) or constant pCO_2 (2300 ppm) with variable T (0–50 °C). White box corresponds to T ± 5 °C from 25 °C, ±500 ppm from 2300 ppm pCO_2: (green box in Fig. 3). (B) Enlargement of area outlined by white box in A. (C) The upper panels show mass of nahcolite precipitated (prec.) (mol/kg of H_2O in initial brine) where T is varied from: (1) 30–20 °C at constant pCO_2 (2300 ppm) (left panel) or (2) pCO_2 is varied from 1800–2800 ppm at constant T (25 °C) (right panel). The lower panels plot nahcolite Ksp (dimensionless equilibrium constant at the appropriate T and pCO_2) (black line—dimensionless) and ion activity product (IAP) [$a\mathrm{Na}{*}a\mathrm{HCO}_3$] (red dotted line—dimensionless) where T is varied from: (1) 30–20 °C at constant pCO_2 (2300 ppm) (left panel) or (2) pCO_2 is varied from 1800–2800 ppm at constant T (25 °C) (right panel). Overlap of lines where nahcolite precipitates as IAP = Ksp. (D) Three-dimensional surface showing mass of nahcolite (moles) precipitated from a volume of Lake Magadi brine containing 1 kg H_2O that was evaporated up to nahcolite saturation at 25 °C, 2300 ppm pCO_2 and then re-equilibrated to various combinations of T (within ± 5 °C) and pCO_2 (within ± 500 ppm). Re-equilibration of nahcolite-saturated brine with lower T and higher pCO_2 will supersaturate this water and precipitate nahcolite with no further evaporative concentration necessary.

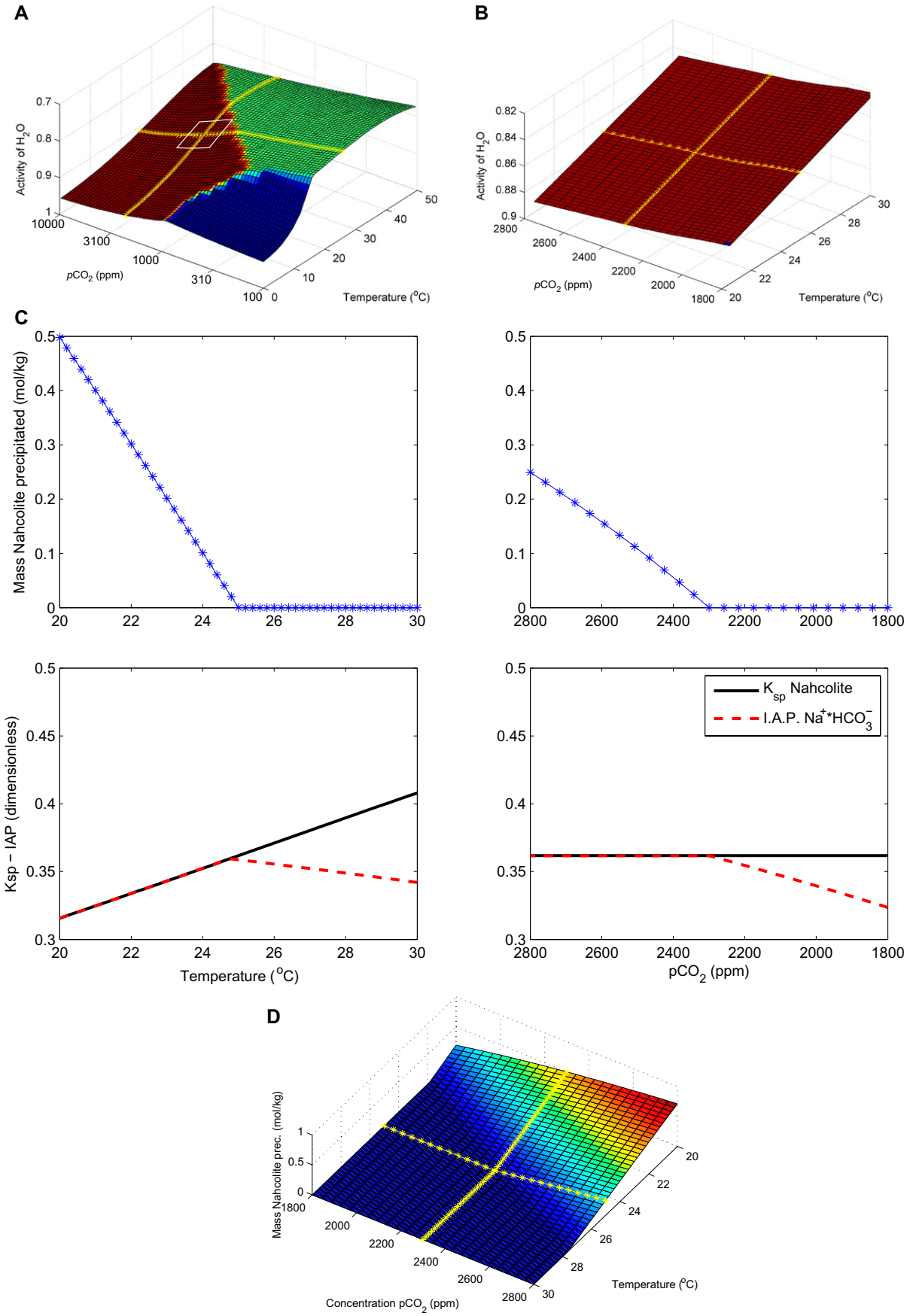

temperature, the more nahcolite is precipitated (upper left panel in Fig. 5C) to keep IAP = Ksp. Likewise, where we increase the pCO_2 from 1800 to 2300 ppm, the IAP increases until IAP = Ksp and nahcolite precipitates (lower right panel in Fig. 5C).

In both situations, lowering T at constant pCO_2, or increasing pCO_2 at constant T, results in nahcolite precipitation without further evaporation. FREZCHEM can also calculate the mass in moles of nahcolite precipitated from a volume of brine containing 1 kg H_2O with changing T or pCO_2. This is shown in the upper panels of Figure 5C. These values for the mass of nahcolite precipitated were calculated as if the T or pCO_2 conditions were changed from 25 to 20 °C (left) and pCO_2 of 2300–2800 ppm (right). For example, if the brine at equilibrium with nahcolite at 25 °C was cooled to 20 °C, ~0.5 moles of nahcolite would precipitate.

FREZCHEM also calculates the saturation state of the brine when both T and pCO_2 are changed (Fig. 5D). Figure 5D shows the same T and pCO_2 range as Figure 5B, but for ease of display, the T scale now decreases from the front of the diagram to the back. The Z axis here is the mass of nahcolite precipitated by an appropriate change in T and pCO_2. Nahcolite is precipitated by lowering T or increasing pCO_2 without any evaporation. The relevance of this experiment to the problem of evaporite focusing in the Green River Formation is apparent. In this case, increasing the temperature of an already evolved brine just at nahcolite saturation leads to dissolution, whereas a temperature decrease causes precipitation, and the greater the decrease in temperature, the more nahcolite is precipitated.

Precipitation of Halite (+ Nahcolite)

The situation becomes more complicated when we consider changing T and pCO_2 of a nahcolite-saturated brine that has just reached halite saturation (the upper surface in Fig. 4 reproduced on its own in Fig. 6A). The yellow lines in Figure 6A again show traces of variable T (0–50 °C) at constant pCO_2 of 2300 ppm, and variable pCO_2 (100–10000 ppm) at constant T (25 °C). The white box in Figure 6A again corresponds to the green box in Figure 3 and is enlarged in Figure 6B. At the center of Figure 6B where the yellow lines cross, the brine is at saturation with nahcolite and halite. There the brine has a unique T, pCO_2, and aH_2O as well as unique concentrations of Na, Cl, K, SO_4, and OH, alkalinity, and a unique pH. Equilibrium thermodynamics fixes the brine composition and that composition will be different from every other point on the surface. The effects of changing T and pCO_2 of this evolved brine on nahcolite and halite saturation state are not at all obvious from this diagram, but instead need to be calculated with FREZCHEM.

Not surprisingly, the effects on nahcolite saturation of: (1) holding T constant and increasing pCO_2, or; (2) holding pCO_2 constant and decreasing T at this low aH_2O (halite saturation) are the same as they were where nahcolite was first precipitated (compare Fig. 6C with Fig. 5C—both with the same vertical scale). Less nahcolite is made at this lower aH_2O (upper left panel in Fig. 6C) than was made at the initial saturation point (upper left panel of Fig. 5C). But again decreasing T or increasing pCO_2 leads to precipitation of nahcolite. However, the effects of decreasing T or increasing pCO_2 on halite precipitation are less obvious.

The lower most panels in Figure 6D show the saturation state of the brine with respect to halite where: (1) temperature changes from 30 to 20 °C at a constant pCO_2 concentration of 2300 ppm (lower left panel) and (2) pCO_2 concentrations change between 1800 and 2800 ppm at a constant temperature of 25 °C (lower right panel). These two experiments correspond to the yellow lines of constant T and constant pCO_2 in Figure 6B. In both lower panels of Figure 6D, the heavy black lines are the Ksp (dimensionless equilibrium constant at the appropriate T and pCO_2 for halite), and the red dotted lines are the ion activity product (IAP—also dimensionless in this case) [$a\mathrm{Na}^+ * a\mathrm{Cl}^-$]. In the case of halite, changing the T at a constant pCO_2 of 2300 ppm only induces halite precipitation at 25 °C (left panels on Fig. 6D, which was, after all, the point where this experiment began). However, decreasing the pCO_2 from 2800 to 1800 ppm at a constant T of 25 °C shows that halite is predicted to precipitate at lower pCO_2 (right panels of Fig. 6D). The path outlined would be obtained if the brine were sequentially equilibrated with lower pCO_2 and the halite was allowed to accumulate (equilibrium crystallization).

Once halite saturation is reached, continued evaporation at a given T and pCO_2 does not dramatically affect the concentrations of Na, Cl, HCO_3, CO_3, and H_2CO_3, because they are controlled by the solubility product constant of halite and nahcolite. In other words, the composition of the evaporating brine is more or less fixed (Fig. 7) with respect to the concentrations of the major ions that form nahcolite and halite (Na^+, Cl^-, $H_2CO_3^o$, HCO_3^-, and CO_3^{2-}). This is seen on Figure 7 where, below ~225 g of water remaining (out of the original 1000 g), all ions except K and SO_4 are constant. The concentrations of K and SO_4 would continue to increase with further evaporation until saturation with a sulfate or potassium salt is reached. Potassium sulfate salts, however, do not occur in the bedded evaporites of the Green River Formation in the Piceance Creek Basin.

The effect of jointly varying T and pCO_2 from 30 to 20 °C and 2800–1800ppm, respectively is shown for nahcolite (Fig. 8A) and halite (Fig. 8B). For ease of display, the T axis now decreases away from the viewer as this orientation better shows the effects of changing T and pCO_2 on halite saturation. Note the different scales on the Z axis of the two diagrams; substantially more nahcolite is made than halite in these experiments by about an order of magnitude. We can summarize the observations at halite saturation as follows. Lowering pCO_2 below 2300 ppm induces precipitation of halite. The mass of halite produced depends on both T and pCO_2. Precipitation of halite and nahcolite can occur from this evolved brine by changing T and pCO_2 with no evaporation. Finally, there is some overlap between the fields for halite and nahcolite precipitation (Figs. 8A and 8B), which is not obvious with the fields displayed for the separate minerals. We shall return to this point below.

The relevance of this experiment to the evaporites in the Parachute Creek Member can be ascertained by considering the four yellow lines on Figures 8A and 8B. These demark constant pCO_2 at 1800, 2050, 2300, and 2550 ppm and, for all four lines, the T varies from 30 to 20 °C. Figure 8C shows the amount of nahcolite (blue lines in the upper tier of panels) and halite (red lines in the lower tier of panels) precipitated at these four pCO_2 concentrations as temperature is varied by ± 5 °C around 25 °C. The original evolved brine was evaporated at a pCO_2 of 2300 ppm, and in this case, as is shown in the third column of panels, lowering the temperature from 25 to 20 °C (as might happen during winter cooling) induces nahcolite precipitation. Conversely, raising the temperature of this system would dissolve nahcolite. At pCO_2 concentrations greater than this 2300 ppm "halite threshold," only nahcolite precipitates with decreasing temperatures, and the higher the pCO_2, the more nahcolite is produced (right-most panels in Fig. 8C). We interpret the laminae of pure nahcolite in Figure 2 to have been produced by cooling of a brine at or above a "halite threshold" pCO_2 (see discussion below). The preservation of pure nahcolite laminae in the thin section implies that the water mass the lamina accumulated in never warmed up enough to become undersaturated with respect to nahcolite.

However, if the original evolved brine that was evaporated at a pCO_2 of 2300 ppm was re-equilibrated with a pCO_2 below the "halite threshold" variable amounts of halite would precipitate in addition to nahcolite. For example, at a pCO_2 of 1800ppm (left-most column in Fig. 8C), lowering the temperature of this brine would induce

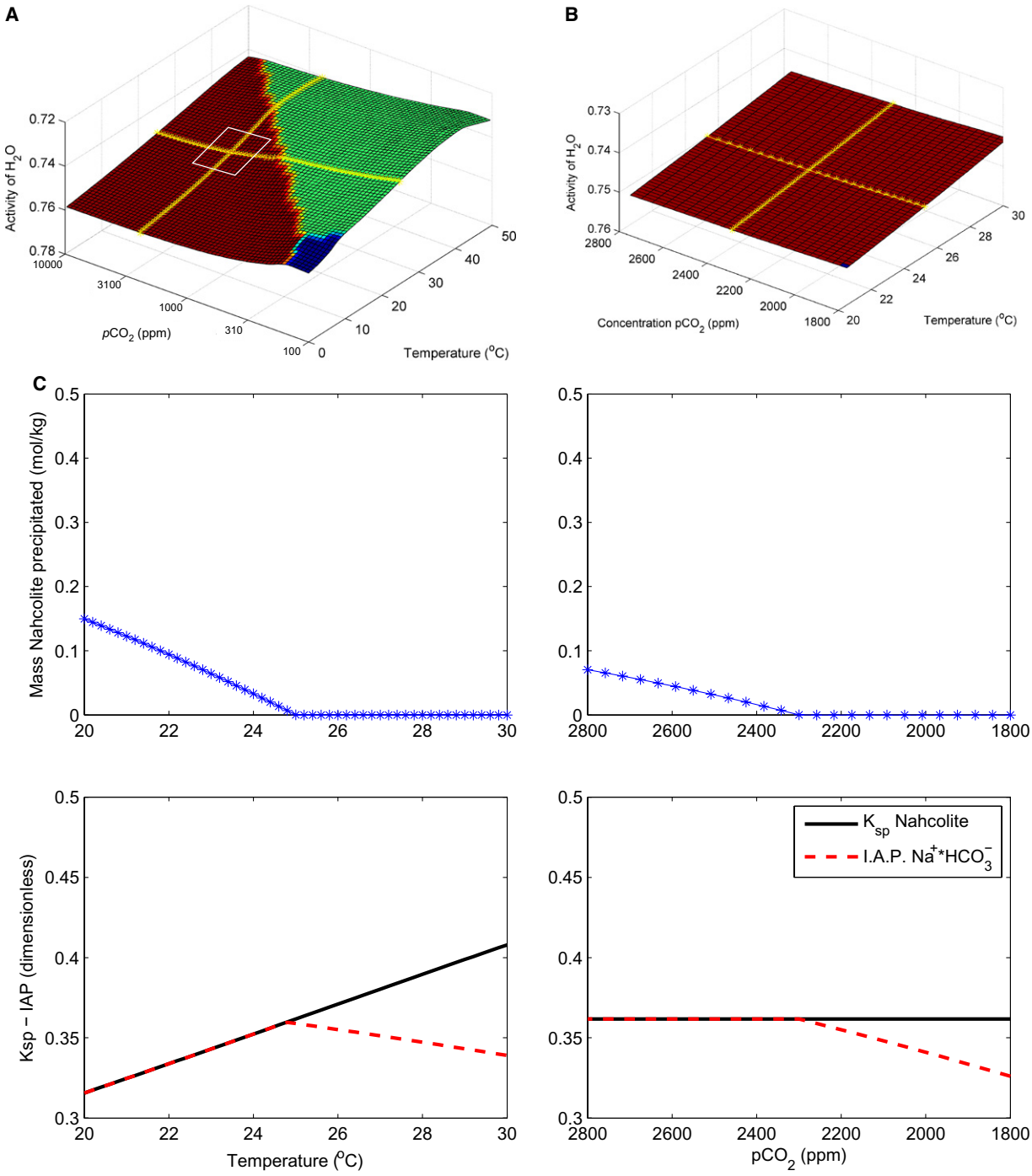

Figure 6 (*on this and following page*). Numerical experiment 1 (green box in Fig. 3): nahcolite + halite saturation. (A) The temperature (T), partial pressure of carbon dioxide (pCO_2), and activity of H_2O conditions of the first appearance of halite + a sodium carbonate phase with evaporation of the Lake Magadi, Kenya, brine (upper surface in Fig. 4). Yellow lines are constant T (25 °C) with variable pCO_2 (100–10,000 ppm) or constant pCO_2 (2300 ppm) with variable T (0–50 °C). White box corresponds to T ± 5 °C from 25 °C, ±500 ppm from 2300 ppm pCO_2: (green box in Fig. 3). (B) Enlargement of area outlined by white box in A. (C) Upper panels plot mass of nahcolite precipitated (mol/kg of H_2O in initial brine) where T is varied from: (1) 30–20 °C at constant pCO_2 (2300 ppm) (left panel) or (2) pCO_2 is varied from 1800–2800 ppm at constant T (25 °C) (right panel). Lower panels in (C) plot nahcolite Ksp (dimensionless equilibrium constant at the appropriate T and pCO_2) (black line—dimensionless) and ion activity product (IAP) [aNa*$a$$HCO_3$] (red dotted line—dimensionless) where T is varied from: (1) 30–20 °C at constant pCO_2 (2300 ppm) (left panel) or (2) pCO_2 is varied from 1800–2800 ppm at constant T (25 °C) (right panel). Overlap of lines where nahcolite precipitates as IAP = Ksp. Lowering the T or increasing the pCO_2 supersaturates the brine with nahcolite with no further evaporative concentration necessary.

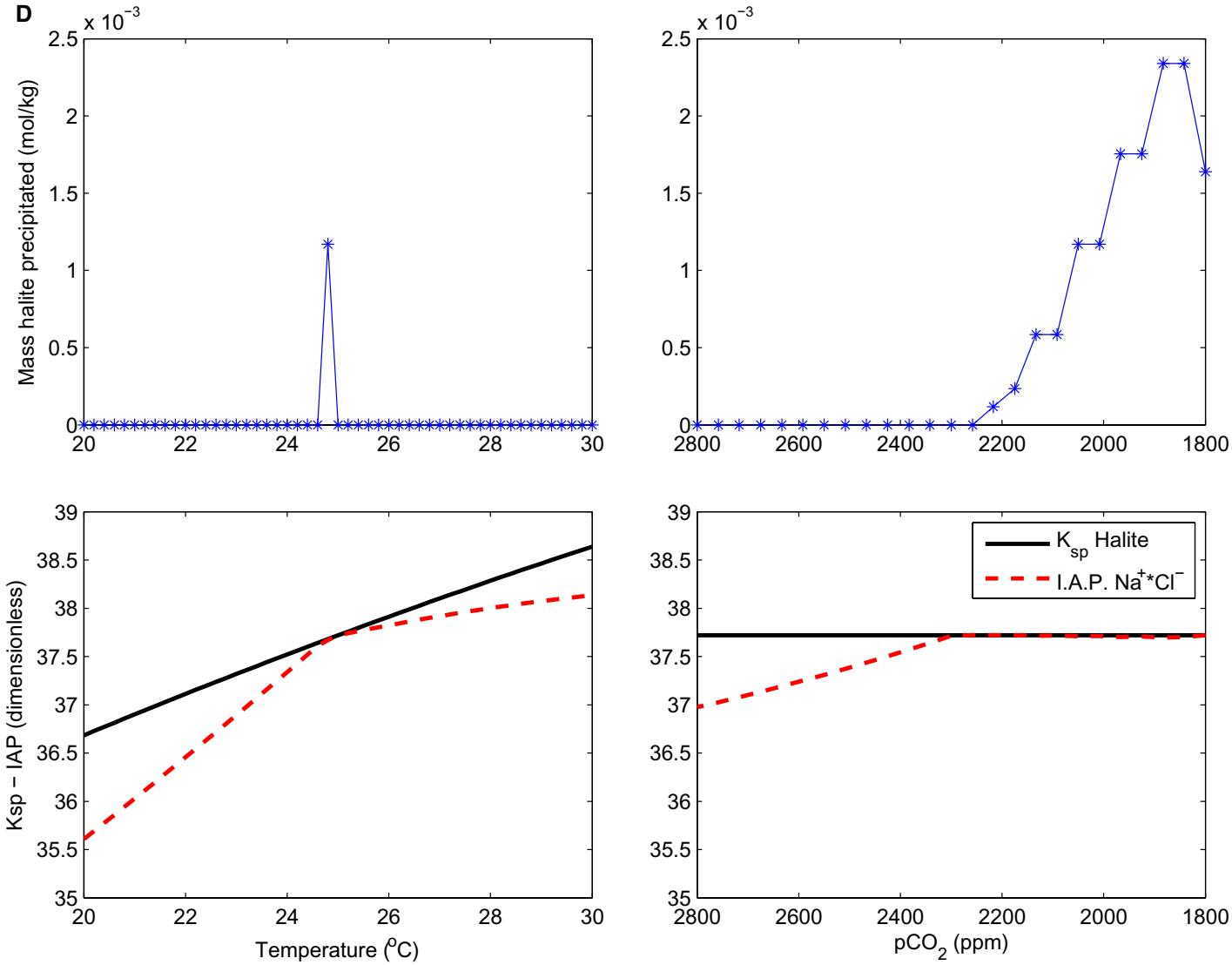

Figure 6 (*Continued*). (D) Upper panels plot mass of halite precipitated (mol/kg of H_2O in the initial brine) where T is varied from: (1) 30–20 °C at constant pCO_2 (2300 ppm) (left panel) or (2) pCO_2 is varied from 1800–2800 ppm at constant T (25 °C) (right panel). Lower panels in (D) plot halite Ksp (black line–dimensionless) and IAP [aNa*aCl] (red dotted line–dimensionless) where T is varied from: (1) 30–20 °C at constant pCO_2 (2300 ppm) (left panel) or (2) pCO_2 is varied from 1800–2800 ppm at constant T (25 °C) (right panel). Overlap of lines where halite precipitates as IAP = Ksp. About an order of magnitude more nahcolite is produced from the same volume of Lake Magadi brine than halite. Lowering the pCO_2 induces halite supersaturation of this brine with no further evaporation needed.

precipitation of halite first (starting at ~26 °C) followed by nahcolite at ~22.5 °C. A number of the lamina in Figure 2 appear to grade from halite up into nahcolite which we interpret to be direct records of sequential cooling. It is important to note that, if the brine did not cool below 22.5 °C, only halite and no nahcolite would precipitate. We interpret laminae of pure halite in Figure 2 to have been produced by this kind of a process. At a pCO_2 intermediate between 1800 and 2300 ppm (2050ppm, Fig. 8C), less halite is produced and more nahcolite is precipitated beginning at ~23.5 °C. Warming the brine would reverse the saturation state and any halite and nahcolite precipitated would dissolve. There is a small temperature overlap where halite and nahcolite co-precipitate. We interpret the laminae composed of mixtures of halite and nahcolite in Figure 2 as precipitating at this overlapping temperature "window" (see below). Figures 9 and 10 are repeats of these numerical experiments with different ranges of T and pCO_2.

The blue box in Figure 3 outlines T at 25–35 °C T range which closely matches the 24–34 °C T range of the modern Dead Sea. At this T range the minimum pCO_2 is 2600 ppm to keep the brine in the nahcolite field throughout its initial evaporative concentration. The pCO_2 concentrations vary from 2600 to 3600 ppm centered on 3100 ppm pCO_2. Figures 9A and 9B are three-dimensional plots that show the masses of nahcolite precipitated under the conditions encompassed by the blue box in Figure 3. Here the original Lake Magadi brine was evaporated to an aH_2O of 0.742 at a T of 25 °C and 2300 ppm pCO_2 (the center of the blue box in Fig. 3). The four yellow lines are lines of constant pCO_2 of 2600, 2850, 3100, and 3750 ppm, respectively, with a T range of 35–25 °C (Fig. 9A). The amounts of nahcolite and halite, produced by T changes if this brine were to re-equilibrate with higher or lower pCO_2 values, are shown in Figure 9C. The upper panels

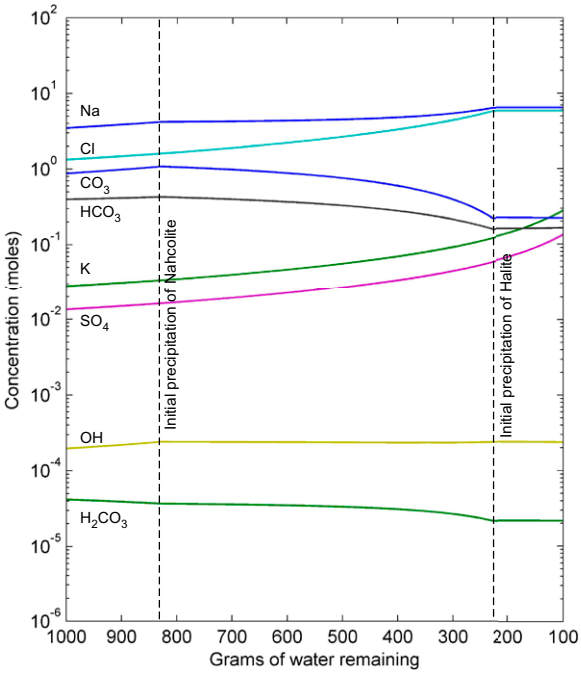

Figure 7. Concentration of major dissolved species where volume of Lake Magadi, Kenya, brine containing 1 kg of H_2O is progressively evaporated. Nahcolite first appears when ~840 g of H_2O remain. Nahcolite continues to precipitate with further evaporation and nahcolite and halite jointly precipitate where <~225 g of H_2O remain. Continued evaporation does not alter the concentration of dissolved Na, Cl, CO_3, HCO_3 and H_2CO_3 or OH.

in Figure 9C show the amount of nahcolite (blue lines) and the lower panels show the amount of halite (red lines) that precipitate under these four different pCO_2 conditions as temperature is varied by ± 5 °C around 30 °C.

In comparison with the conditions of the first experiment (30–20 °C, 1800–2800 ppm pCO_2) at these higher T and pCO_2 values about the same mass of nahcolite is precipitated above the "halite threshold" at a pCO_2 ≥3100 ppm. Below 3100 ppm, slightly more halite and nahcolite are produced, but the overlap in T where halite and nahcolite both forms is substantially increased. This is most clearly seen in Figure 11, map views of the respective T and pCO_2 ranges of the three experiments. Experiment 1 is the central panel and experiment 2 is mapped in the lower panel. In these plots, blue asterisks indicate nahcolite precipitation and red circles show halite crystallization. The zone of overlap increases with increasing T and pCO_2.

The red box in Figure 3 outlines T conditions ± 5 °C around 17 °C: a T range of 22–12 °C. These are the lowest T conditions possible to stay in the nahcolite field; they fix the minimum pCO_2 at 1000 ppm. For this experiment, pCO_2 concentrations vary from 1000 to 2000 ppm with initial evaporation at 1500 ppm pCO_2. Figures 10A and 10B show the masses of nahcolite precipitated under these conditions. The four yellow lines are lines of constant pCO_2 of 1000, 1250, 1500, and 1750 ppm, respectively. Figure 10C shows the amounts of nahcolite (blue lines at top) and halite (red lines at bottom) produced by T changes if this brine were to re-equilibrate with higher or lower pCO_2 values. In comparison with the conditions of experiment 1 (30–20 °C, 1800–2800 ppm pCO_2) the lower T and pCO_2 values of experiment 3 produce the same mass of nahcolite above the "nahcolite threshold" at a pCO_2 ≥1500 ppm. Below 1500 ppm, slightly less halite and nahcolite are produced. The temperature overlaps at which halite and nahcolite both form decreases, as seen in Figure 11 comparing the upper panel to the other two.

EVAPORITE FOCUSING MODEL: APPLICATION TO THE GREEN RIVER FORMATION IN THE PICEANCE CREEK BASIN

Application of the FREZCHEM simulations to the Parachute Creek Member is straightforward. During warm summer periods, the higher solubility of nahcolite and halite at higher temperatures induced dissolution of these phases and counteracted any possible reversal toward lowered solubility caused by increased evaporation. As brines cooled in winter, halite, nahcolite or both crystallized depending on the pCO_2 in the lake water during cooling. As T dropped to a winter low of 20–25 °C, the dissolved carbon dioxide content in various parts of the lake and the lowest winter T obtained determined whether halite, nahcolite, or both precipitated (Fig. 2). Then, in the summer, where the lake bottom was above the thermocline, any winter-precipitated halite and nahcolite dissolved and recycled back into the lake brine. The evaporite layer precipitated during the winter (nahcolite, halite, or nahcolite + halite) was only preserved in the deep parts of the lake below the thermocline.

The implications for this model are profound. First, the distribution of evaporites in the Parachute Creek Member in the Piceance Creek Basin records the deepest portion of the basin—the area below the thermocline. Instead of being dissolved much later in the history of the basin by infiltrating ground waters, nahcolite and halite layers above the thermocline were dissolved contemporaneously over most (at least 85% of the current area of preserved oil shales) of the Piceance Creek Basin (Fig. 1). In this evaporite focusing scenario, variations in thickness and extent of the nahcolite layers detailed by Brownfield et al. (2010a, 2010b) reflect how the deepest part of the basin shifted location with time. The question then arises as to the depth of the thermocline in the paleolake that filled the Piceance Creek Basin. In the modern Dead Sea, the thermocline is at ~25 m in the summer and dissipates in winter when the Dead Sea becomes isothermal. The modern Dead Sea has a considerably smaller surface area than the lake that filled the Piceance Creek Basin. Two modern saline lakes with areas on the order of 4500 km^2 (the current area of the eroded remnant deposits of that lake) are the Great Salt Lake (~4600 km^2) in Utah, USA and Qinghai Lake (~4500 km^2) in western China. All modern lakes not directly on the equator undergo annual surface temperature variations and, if deep enough, stratify (Boehrer and Schultze, 2008), and there is no reason to suspect that this was not the case in the Eocene. Although the climate of the Piceance Creek Basin was apparently subtropical (like the modern Dead Sea), the Piceance Creek Basin lake was at ~39–40°N latitude (Smith et al., 2008; Jagniecki et al., 2015). Circulation in the Great Salt Lake (maximum depth varies but is on the order of 15 m) is complicated by the causeway that cut off the North Arm in ~1960 CE. The summer thermocline in the Great Salt Lake has been measured at ~10 m depth (Wurtsbaugh and Berry, 1990). In Qinghai Lake (maximum depth ~30 m) the summer thermocline has been measured between 15–20 m depth (Williams, 1991). Neither lake is an exact climatic match with the lake that filled the Piceance Basin, but both lakes develop significant summer thermoclines. We therefore estimate that the summer thermocline in the paleolake that filled the Piceance Creek Basin was on the order of 15–25 m deep.

A second important implication of this model is that, in this scenario of winter precipitation and summer re-dissolution, the overall mass of dissolved solutes in the lake remains relatively constant. Only a relatively small amount of dissolved Na^+, Cl^-, and ions that contribute to alkalinity ($H_2CO_3 + HCO_3^- + CO_3^{2-}$) were permanently

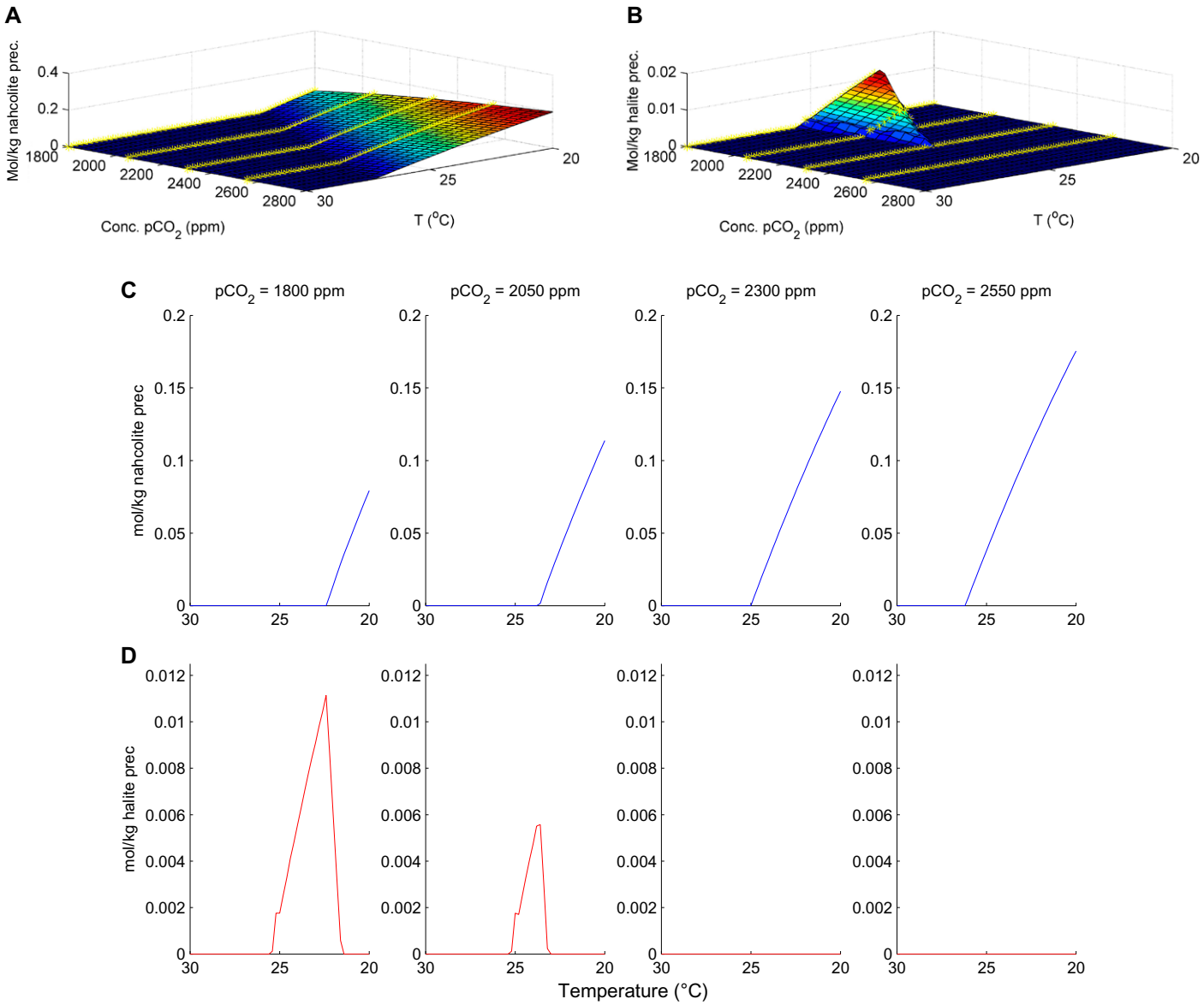

Figure 8. Numerical experiment 1 (green box in Fig. 3): nahcolite + halite saturation. (A) Three-dimensional surface showing mass of nahcolite (moles) precipitated (prec.) from a volume of Lake Magadi, Kenya, brine containing 1 kg of H_2O that was evaporated up to nahcolite + halite saturation at 25 °C, 2300 ppm partial pressure of carbon dioxide (pCO_2) and then re-equilibrated to various combinations of temperature (T) (within ± 5 °C) and pCO_2 (within ± 500 ppm). The yellow lines are 30–20 °C changes in T at four different, constant pCO_2 values: 1800, 2050, 2300, and 2550 ppm. (B) Three-dimensional surface showing mass of halite (moles) precipitated from same brine as in A, re-equilibrated to the same combinations of T and pCO_2. The yellow lines denote the same T and pCO_2 conditions as in A. (C) Masses of nahcolite precipitated from a volume of Lake Magadi water containing 1 kg H_2O as T changes from 30–20 °C under various constant pCO_2 values (yellow lines in A). (D) Masses of halite precipitated from same brine when T changes from 30–20 °C under constant pCO_2 values (yellow lines in B). See text for further details.

taken out of the lake water over an annual cycle. The small mass of dissolved ions removed over an annual cycle must have been replaced by inflow waters to build up the tens of meters thick sequence of nahcolite + halite interbedded with oil shales in the center of the basin (Fig. 1B). The variation in evaporite mineralogy at the lamination scale in the Parachute Creek Member is the result of variations in the dissolved carbon dioxide content and temperature of various reservoirs. Variations in thickness of evaporite laminae probably represent different amounts of summer evaporation which was not considered in this modeling. Any evaporation would increase the concentration of the ions in the Piceance Creek Basin brine lake; more evaporation would produce a greater mass and thicker evaporite layer when the lake cooled during the following winter.

DISCUSSION AND CONCLUSIONS

The numerical experiments described here allow some inferences about conditions in the paleolake that filled the Piceance Creek Basin. First, the lake was thermally stratified with substantial (~10 °C) changes in T of the water mass above the deep coldest waters below the thermocline. Second, different portions of the lake must have had

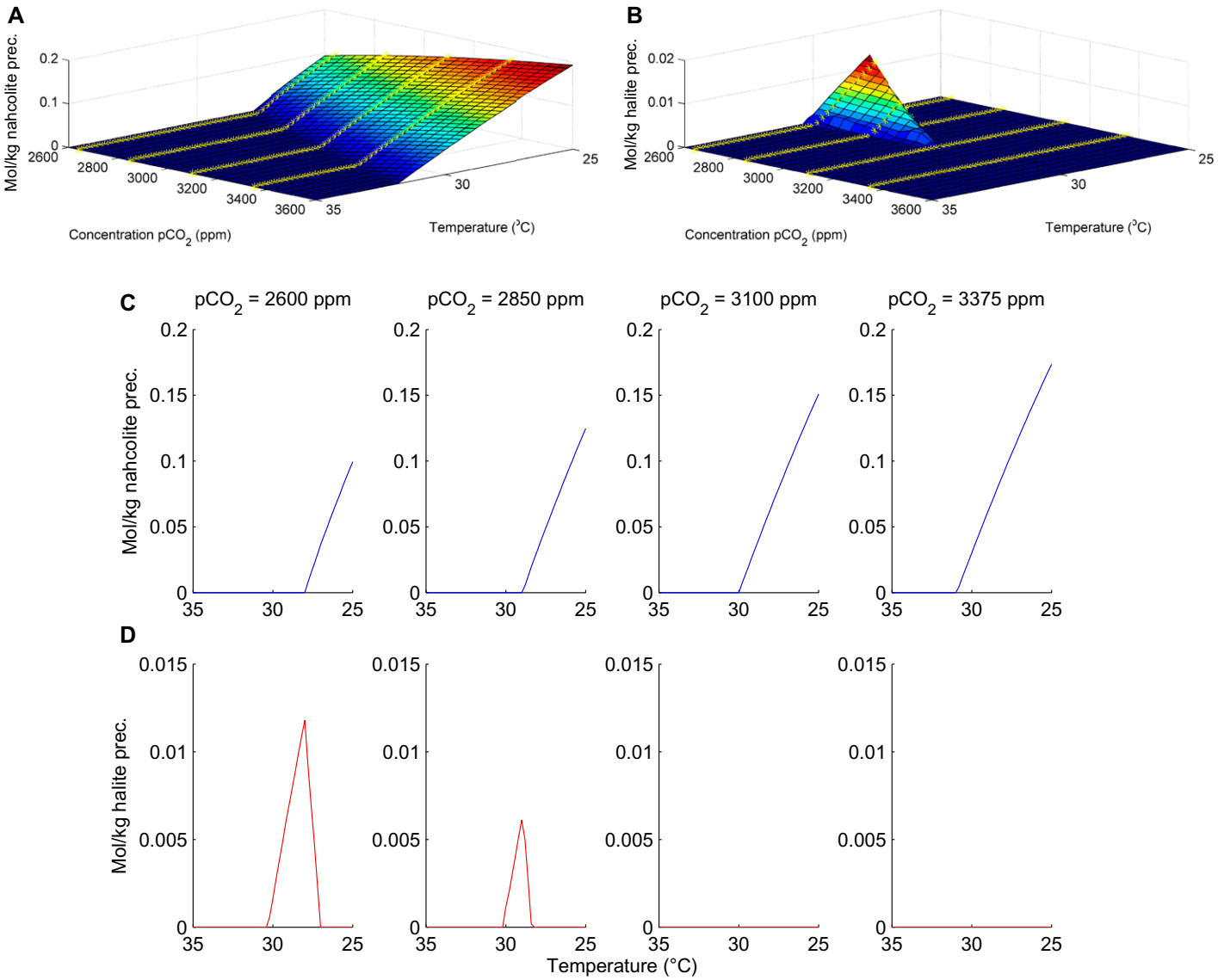

Figure 9. Numerical experiment 2 (blue box in Fig. 3): nahcolite + halite saturation. (A) Three-dimensional surface showing mass of nahcolite (moles) precipitated (prec.) from a volume of Lake Magadi, Kenya, brine containing 1 kg of H_2O that was evaporated up to nahcolite + halite saturation at 30 °C, 3100 ppm partial pressure of carbon dioxide (pCO_2) and then re-equilibrated to various combinations of temperature (T) (within ± 5 °C) and pCO_2 (within ± 500 ppm). The yellow lines are 35–25 °C changes in T at four different, constant pCO_2 values: 2600, 2850, 3100, and 3750 ppm. (B) Three-dimensional surface showing mass of halite (moles) precipitated from same brine as in A, re-equilibrated to the same combinations of T and pCO_2. The yellow lines denote the same T and pCO_2 conditions as in A. (C) Masses of nahcolite precipitated from a volume of Lake Magadi water containing 1 kg H_2O as T changes from 35 to 25 °C under various constant pCO_2 values (yellow lines in A). (D) Masses of halite precipitated from the same brine when T changes from 35 to 25 °C under constant pCO_2 values (yellow lines in B). See text for further details.

different pCO_2 with halite precipitating from the waters with the lowest dissolved CO_2, nahcolite precipitating from the waters with the highest dissolved CO_2, and mixtures of halite and nahcolite in waters with intermediated levels of dissolved CO_2. These implications are clear outcomes of the "evaporite focusing" model presented here.

One obvious question is, where in the lake were the different water masses with varying pCO_2? Many of the halite layers in cores from the center of the basin contain flattened halite rafts (Fig. 2) that grew at the air-water interface where they were buoyed up by surface tension during growth. Thermodynamic calculations suggested that the partial pressure of dissolved carbon dioxide in modern saline lakes is significantly higher than in the atmosphere, and that CO_2 diffuses out of these lakes into the atmosphere (Duarte et al. 2008; Raymond et al. 2013). The sparse measurements of pCO_2 in saline lakes shows it to be higher than atmospheric (Oxburgh et al., 1991; Golan et al., 2016). The lowest pCO_2 in a lake degassing carbon dioxide to the atmosphere would be the surface waters and the halite rafts in the evaporites of the Green River Formation in the Piceance Creek Basin support the idea that the surface waters were the water mass with the lowest pCO_2. Extraction of CO_2 by photosynthetic organisms would also lower near surface pCO_2 in the lake. Bottom growth halite crystals

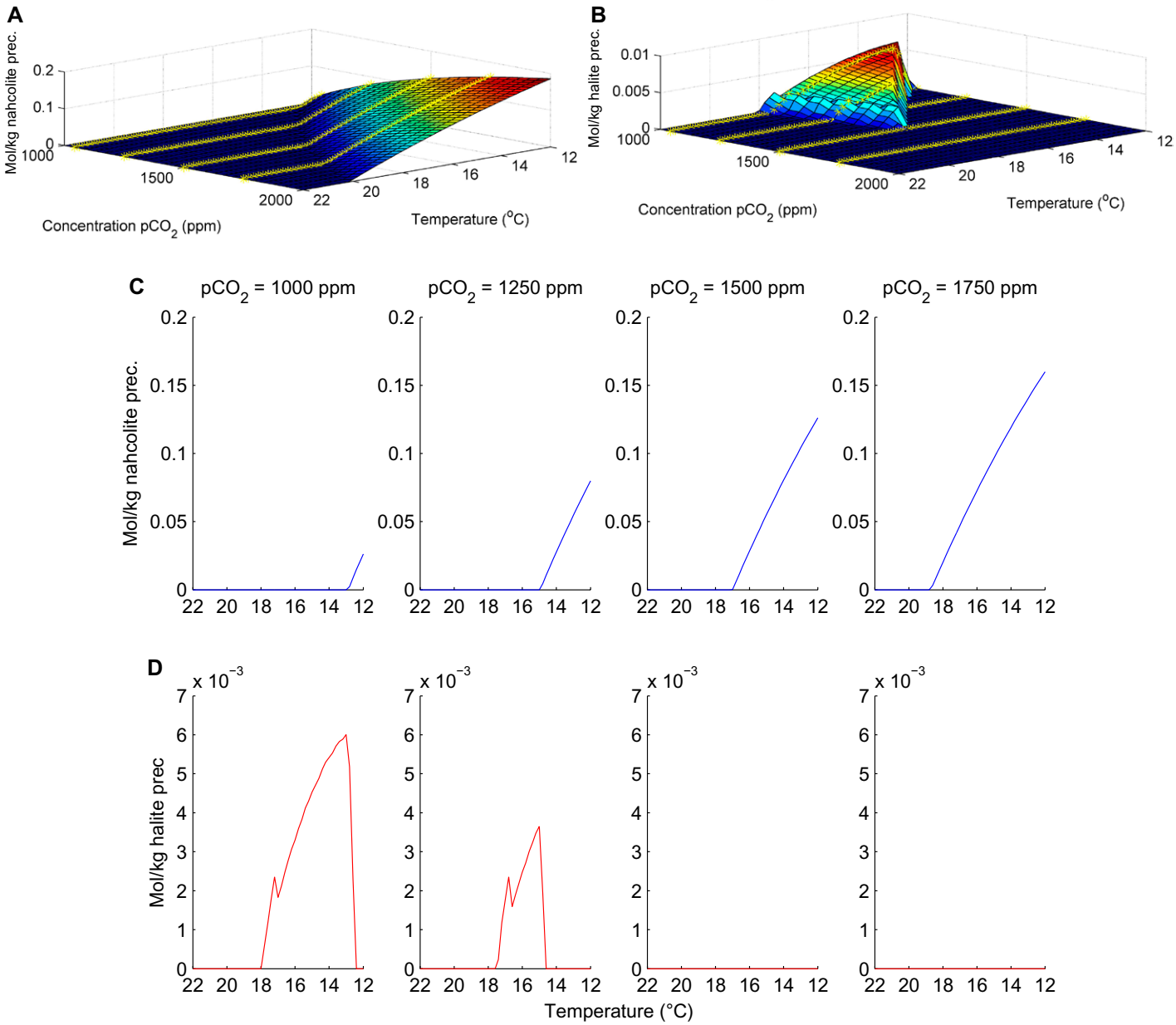

Figure 10. Numerical experiment 3 (red box in Fig. 3): nahcolite + halite saturation. (A) Three-dimensional surface showing mass of nahcolite (moles) precipitated (prec.) from a volume of Lake Magadi, Kenya, brine containing 1 kg of H_2O that was evaporated up to nahcolite + halite saturation at 17 °C, 1500 ppm partial pressure of carbon dioxide (pCO_2) and then re-equilibrated to various combinations of temperature (T) (within ± 5 °C) and pCO_2 (within ± 500 ppm). The yellow lines are 12–22 °C changes in T at four different, constant pCO_2 values: 1000, 1250, 1500, and 1750 ppm. (B) Three-dimensional surface showing mass of halite (moles) precipitated from the same brine as in A, re-equilibrated to the same combinations of T and pCO_2. The yellow lines denote the same T and pCO_2 conditions as in A. (C) Masses of nahcolite precipitated from a volume of Lake Magadi water containing 1 kg H_2O as T changes from 22–12 °C under various constant pCO_2 values (yellow lines in A). (D) Masses of halite precipitated from the same brine when T changes from 22–12 °C under constant pCO_2 values (yellow lines in B). See text for further details.

are common in the bedded evaporites of the basin center (Fig. 2) but bottom growth nahcolite crystals have not been reported. This implies that the waters below the thermocline were, from time to time, very slightly saturated with halite, but at or slightly below saturation with nahcolite. This, in turn, suggests that the waters below the thermocline had a dissolved carbon dioxide content at the "halite threshold": higher than the surface waters but not high enough to allow precipitation of nahcolite. The waters with the highest pCO_2 in the lake that filled the Piceance Creek Basin then were sandwiched between the surface waters and the thermocline. In many lakes, aerobic respiration (which consumes oxygen and produces carbon dioxide) takes place throughout the water column and is the main source of dissolved CO_2 in lake waters (Bridge and Demicco, 2008). It is clear that in the Piceance Basin, lacustrine production of organic matter exceeded the ability of microbes to consume it. The position of

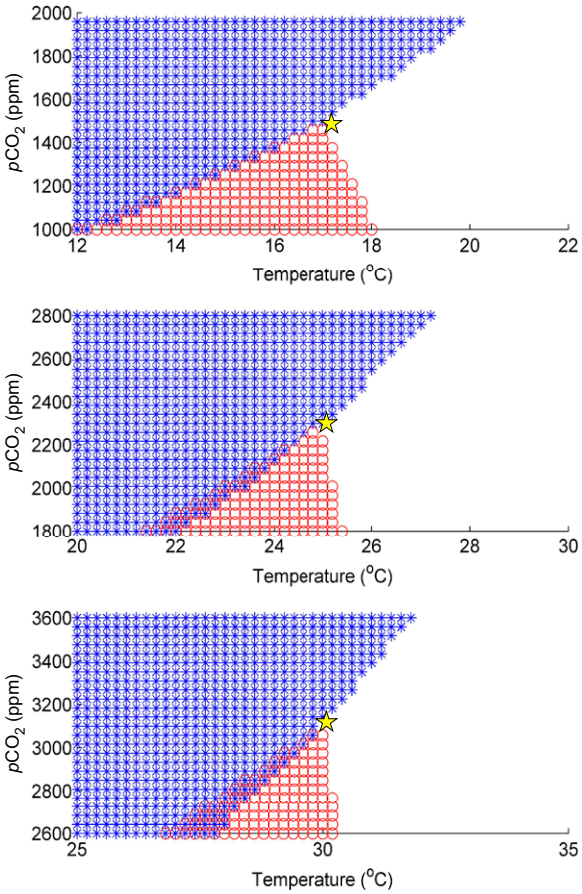

Figure 11. Temperature (T) versus partial pressure of carbon dioxide (pCO_2) plots of precipitation of nahcolite (blue asterisks), halite (red circles), and nahcolite + halite (both symbols) for the three experiments outlined in Figure 3. Yellow stars show the temperature (T) and partial pressure of carbon dioxide (pCO_2) conditions of evaporation up to initial nahcolite + halite saturation. This is also the "halite threshold" for each experiment (combination of pCO_2 and T where halite and nahcolite are exactly at saturation). Zone where nahcolite and halite co-precipitate increases with increasing pCO_2 and T. See text for further details.

the boundary between aerobic, CO_2-producing microbial respiration and anerobic microbial H_2S production then was somewhere within our 25 m estimate of the depth to the thermocline. The highest dissolved CO_2 then would be below the surface layer and above the aerobic/anaerobic boundary.

These numerical experiments were intended as a theoretical exercise aimed at understanding: (1) the restriction of evaporites in the Piceance Creek Basin to the center of the basin without recourse for later wholesale dissolution of bedded evaporites and (2) explaining the variable mineralogy of the bedded evaporites in terms of changing T and pCO_2 without recourse to changing the chemistry of the lake waters by adding new ions and then saturating the lake by evaporation. On the first point, there is no evidence of wholesale dissolution of evaporites in the basin. On the second point, the composition of the paleolake was buffered against even small changes in composition by its sheer volume, yet the thicknesses and compositions of preserved evaporite laminae are highly variable. This "evaporite focusing" mechanism is based on "halite focusing" described from the modern Dead Sea. In the Dead Sea halite precipitates during cold winter months and re-dissolves above the thermocline at ~25 m depth upon summer warming. In the lake that filled the Piceance Creek Basin, in addition to summer and winter cooling, variable carbon dioxide content in different parts of the highly concentrated brines affected halite and the sodium carbonate mineral deposited from those brines. These experiments show that, depending on the CO_2 content of the brines, only halite, only nahcolite, or various mixtures of the two minerals can be produced. Preservation of these minerals would be focused below the thermocline in deeper portions of the basin. This modeling suggests that most of the ancient lake that filled the Eocene basin in Colorado was <25 m deep through much of its history—judging by the depth to the thermocline in the modern Dead Sea and Qinghai Lake. Our original experimental conditions (30–20 °C, 1800–2800 ppm pCO_2) are reasonable estimates for the conditions in the paleolake that filled the Piceance Creek Basin in light of the fluid inclusion temperatures reported by LaClair and Lowenstein (2009).

Finally, there are other instances where evaporites that occur in the center of a basin do not extend out to the edges of the basin (Hsü et al., 1973; Dyni, 1981; Lowenstein, 1988). The possibility that evaporite focusing caused by summer-winter T changes in the solubility of the minerals should be considered for any evaporite deposit that has this characteristic and formed in a perennial brine body.

ACKNOWLEDGMENTS

Funding was provided by National Science Foundation, Integrated Earth Systems grant EAR-1812741. The suggestions of two anonymous reviewers improved the manuscript. Earlier drafts of the manuscript and illustrations were reviewed by Elliot Jagniecki, Joseph Janick, and Dave Jenkins.

REFERENCES CITED

Boehrer, B., and Schultze, M., 2008, Stratification of lakes: Reviews of Geophysics, v. 46, 27 p., https://doi.org/10.1029/2006RG000210.

Bridge, J.S., and Demicco, R.V., 2008, Earth Surface Processes, Landforms and Sediment Deposits: Cambridge, UK, Cambridge University Press, 814 p., https://doi.org/10.1017/CBO9780511805516.

Brownfield, M.E., Mercier, T.J., Johnson, R.C., and Self, J.G., 2010a, Nahcolite resources in the Green River Formation, Piceance Basin, Colorado, *in* U.S. Geological Society Oil Shale Assessment Team, ed., Oil Shale and Nahcolite Resources of the Piceance Basin, Colorado: United States Geological Survey Digital Data Series 69-Y, 51 p.

Brownfield, M.E., Johnson, R.C., and Dyni, J.R., 2010b, Sodium carbonate resources of the Eocene Green River Formation, Uinta Basin, Utah and Colorado, *in* U.S. Geological Society Oil Shale Assessment Team, ed., Oil Shale and Nahcolite Resources of the Piceance Basin, Colorado: United States Geological Survey Digital Data Series 69-BB, 13 p.

Duarte, C.M., Prairie, Y.T., Contes, C., Cole, J.J., Striegl, R., Melack, J., and Downing, J.A., 2008, CO_2 emissions from saline lakes: A global estimate of a surprisingly large flux: Journal of Geophysical Research. Biogeosciences, v. 113, no. G4, https://doi.org/10.1029/2007JG000637.

Dyni, J.R., 1981, Geology of the nahcolite deposits and associated oil shales of the Green River Formation in the Piceance Creek Basin, Colorado [Ph.D. thesis]: Boulder, Colorado, USA, University of Colorado, 144 p.

Dyni, J.R., 1996, Sodium carbonate resources of the Green River Formation in Utah, Colorado, and Wyoming: United States Geological Survey Open-File Report 96-729, 39 p.

Eugster, H.P., 1966, Sodium carbonate-bicarbonate minerals as indicators of pCO_2: Journal of Geophysical Research, v. 71, p. 3369–3377, https://doi.org/10.1029/JZ071i014p03369.

Eugster, H.P., 1970, Chemistry and origin of the brines of Lake Magadi, Kenya: Mineralogical Society of America Special Paper, v. 3, p. 213–235.

Golan, R., Gavrieli, I., Ganor, J., and Lazar, B., 2016, Controls on the pH of hyper-saline lakes: A lesson from the Dead Sea: Earth and Planetary Science Letters, v. 434, p. 289–297, https://doi.org/10.1016/j.epsl.2015.11.022.

Hardie, L.A., and Eugster, H.P., 1970, The evolution of closed-basin brines, *in* Morgan, B.A., ed., Mineralogical Society of America 50th Anniversary Symposia: Mineralogical Society of America Special Publication, v. 3, p. 273–290.

Hsü, K.J., Ryan, W.B.F., and Cita, M.B., 1973, Late Miocene desiccation of the Mediterranean: Nature, v. 242, p. 240–244, https://doi.org/10.1038/242240a0.

Jagniecki, E.A., and Lowenstein, T.K., 2015, Evaporites of the Green River Formation, Bridger and Piceance Creek Basins: Deposition, diagenesis, paleobrine chemistry and Eocene atmospheric CO2, *in* Smith, M.E., and Carroll, A.R., eds, Stratigraphy and Paleolimnology of the Green River Formation, Western USA: Syntheses in Limnogeology: Dordrecht, The Netherlands, Springer, p. 277–312.

Jagniecki, E.A., Lowenstein, T.K., Jenkins, D.M., and Demicco, R.V., 2015, Eocene atmospheric CO_2 from the nahcolite proxy: Geology, v. 43, p. 1075–1078.

Johnson, R.C., and Brownfield, M.E., 2015, Development, evolution, and destruction of the saline mineral area of Eocene Lake Uinta, Piceance Basin, western Colorado: United States Geological Survey Scientific Investigations Report 2013-5176, 76 p., 2 pl., https://doi.org/10.3133/sir20135176.

Jones, B.F., Eugster, H.P., and Rettig, S.L., 1977, Hydrochemistry of the Lake Magadi basin, Kenya: Geochimica et Cosmochimica Acta, v. 41, p. 53–72, https://doi.org/10.1016/0016-7037(77)90186-7.

LaClair, D., and Lowenstein, T.K., 2009, Fluid inclusion microthermometry from halite in the Eocene Green River Formation, Piceance Creek basin, Colorado, USA: Evidence for a perennial stratified saline lake: Geological Society of America Abstracts with Programs, v. 41, no. 7, p. 512.

Lowenstein, T.K., 1988, Origin of depositional cycles in a Permian "saline giant": The Salado (McNutt zone) evaporites of New Mexico and Texas: Geological Society of America Bulletin, v. 100, p. 592–608, https://doi.org/10.1130/0016-7606(1988)100<0592:OODCIA>2.3.CO;2.

Lowenstein, T.K., and Demicco, R.V., 2006, Elevated Eocene atmospheric CO_2 and its subsequent decline: Science, v. 313, p. 1928, https://doi.org/10.1126/science.1129555.

Lowenstein, T.K., Jagniecki, E.A., Carroll, A.R., Smith, M.E., Renaut, R.W., and Owen, R.B., 2017, The Green River salt mystery: What was the source of the hyperalkaline lake waters?: Earth-Science Reviews, v. 173, p. 295–306, https://doi.org/10.1016/j.earscirev.2017.07.014.

Marion, G.M., 2001, Carbonate mineral solubility at low temperatures in the Na-K-Mg-Ca-H-Cl-OH-HCO_3-CO_3-CO_2-H_2O system: Geochimica et Cosmochimica Acta, v. 65, p. 1883–1896, https://doi.org/10.1016/S0016-7037(00)00588-3.

Oxburgh, R., Broecker, W.S., and Wanninkhof, R.H., 1991, The carbon budget of Mono Lake: Global Biogeochemical Cycles, v. 5, p. 359–372, https://doi.org/10.1029/91GB02475.

Raymond, P.A., Hartmann, J., Lauerwald, R., Sobek, S., McDonald, C., Hoover, M., Butman, D., Striegl, R., Mayorga, E., Humborg, C., Kortelainen, P., Dürr, H., Meybeck, M., Ciais, P., and Guth, P., 2013, Global carbon dioxide emissions from inland waters: Nature, v. 503, p. 355–359, https://doi.org/10.1038/nature12760 (erratum: http://dx.doi.org/10.1038/nature13142).

Risacher, F., and Clement, A., 2001, A computer program for the simulation of evaporation of natural waters to high concentration: Computers & Geosciences, v. 27, p. 191–201, https://doi.org/10.1016/S0098-3004(00)00100-X.

Sirota, I., Arnon, A., and Lensky, N.G., 2016, Seasonal variations of halite saturation in the Dead Sea: Water Resources Research, v. 52, p. 7151–7162, https://doi.org/10.1002/2016WR018974.

Sirota, I., Enzel, Y., and Lensky, N.G., 2017, Temperature seasonality control on modern halite layers in the Dead Sea: In situ observations: Geological Society of America Bulletin, v. 129, p. 1181–1194.

Sirota, I., Enzel, Y., and Lensky, N.G., 2018, Halite focusing and amplification of salt thickness: From the Dead Sea to deep hypersaline basins: Geology, v. 46, p. 851–854, https://doi.org/10.1130/G45339.1.

Smith, M.E., Carroll, A.R., and Singer, B.S., 2008, Synoptic reconstruction of a major ancient lake system: Eocene Green River Formation, western United States: Geological Society of America Bulletin, v. 120, p. 54–84, https://doi.org/10.1130/B26073.1.

Tänavsuu-Milkeviciene, K., and Sarg, J.F., 2012, Evolution of an organic-rich lake basin: Stratigraphy, climate and tectonics: Piceance Creek basin, Eocene Green River Formation: Sedimentology, v. 59, no. 6, p. 1735–1768, https://doi.org/10.1111/j.1365-3091.2012.01324.x.

Williams, W.D., 1991, Chinese and Mongolian saline lakes: A limnological overview: Hydrobiologia, v. 210, p. 39–66, https://doi.org/10.1007/BF00014322.

Wurtsbaugh, W.A., and Berry, T.S., 1990, Cascading effects of decreased salinity on the plankton, chemistry and physics of the Great Salt Lake (Utah): Canadian Journal of Fisheries and Aquatic Sciences, v. 47, p. 100–109, https://doi.org/10.1139/f90-010.

Science Editor: Bradley S. Singer
Associate Editor: Michael Smith

Manuscript Received 29 March 2019
Revised Manuscript Received 23 July 2019
Manuscript Accepted 28 August 2019

Printed in the USA